PHYSICAL REVIEW VOLUME 161, NUMBER 3 15 SEPTEMBER 1967

Longitudinal and Transverse Optical Lattice Vibrations in Quartz

J. F. Scott and S. P. S. Porto
Bell Telephone Laboratories, Murray Hill, New Jersey

(Received 27 March 1967)

The vibrational Raman spectrum of quartz has been obtained by means of argon laser excitation. Vibrations ascribed by earlier investigators to multiphonon processes are shown to be longitudinal components of the doubly degenerate species-E vibrations. The frequency splittings observed between the longitudinal and transverse components of each species-E mode are shown to agree very well with the values calculated using classical oscillator theory. The frequency and symmetry of each of the vibrations in α-quartz are correlated with those of β-quartz. A discussion of the complications introduced by birefringence and anisotropy is also presented. It is shown that frequency splittings between longitudinal and transverse vibrations due to electrostatic forces are in some cases much greater for quartz than the frequency shifts due to the anisotropy of the short-range interatomic forces, contrary to what has been concluded previously in the literature.

INTRODUCTION

ALTHOUGH the phonon spectrum of quartz has been studied extensively[1–5] in the past by means of both infrared and Raman techniques, renewed experimental study of this crystal is important for several reasons. First, quartz is uniaxial, ionic, and birefringent. Uniaxial crystals are of maximum interest at present because the theory of the first-order spectra of cubic crystals has been worked out in detail, while that of biaxial crystals has not yet been attacked; that of uniaxial crystals is in an active state of development. Uniaxial ionic crystals are expected to exhibit frequency shifts due to anisotropy of short-range interionic forces and also shifts due to long-range electrostatic forces. It is not known *a priori* which of these two effects predominates in a given crystal; this determination requires detailed experimental study. Second, quartz is complex. The theories pretaining to first-order phonon spectra in uniaxial crystals have generally been developed for diatomic lattices; it is of particular interest to examine their extension to more complex crystals, such as quartz, which has nine atoms per unit cell and, consequently, several different phonon modes. Third, quartz undergoes a phase change at an easily accessible temperature (575°K), and both phases have been considered previously with respect to group-theory and normal-mode analyses. This permits correlation of phonon characteristics above and below the transition temperature. Fourth, previous assignments of the spectral features observed for quartz are varied and inconsistent and have not considered some aspects of contemporary theory. Fifth, accurate indentification of the first-order spectrum is requisite for the development of polariton theory—a topic of current interest—for a given crystal (a separate paper on the spectrum of these mixed electromagnetic-mechanical excitations in quartz is forthcoming).

We shall show that the "extra" lines in the quartz spectrum are not multiphonon processes, as proposed by most of the earlier workers, but are the longitudinal vibrations. We shall use classical oscillator theory to calculate the frequencies of these longitudinal modes, and we shall show that our experimental results agree very well with our theoretical calculations. The orientation-dependent frequency shifts are interpreted as the effects of anisotropy and are consistent with the theoretically predicted dependence upon the angle between the c axis of the crystal and the direction of phonon propagation. Correlation of the results of the analysis of α-quartz with that of β-quartz will also be made, showing the effect the phase transition has upon the symmetry of the normal modes.

THEORY

Discussions of the ordinary Raman effect have been given by Placzek,[6] Huang,[7] Menzies,[8] and, recently, Loudon.[9] It is convenient to summarize here some of the theoretical relationships which facilitate experimental analysis. For the vibrational Raman process in crystals, a photon of energy $h\nu_i$ and momentum $\mathbf{k}_i$ incident upon the crystal is inelastically scattered. It is annihilated at the scattering center, exciting a mechanical lattice vibration (phonon) of energy $h\nu_p$ and momentum $\mathbf{k}_p$ and an emission photon (Stokes wave) of energy $h\nu_s$ and momentum $\mathbf{k}_s$. Conservation of energy and momentum requires that

$$h\nu_i = h\nu_p + h\nu_s \tag{1}$$

or

$$\omega_i = \omega_p + \omega_s\,, \tag{2}$$

and

$$\mathbf{k}_i = \mathbf{k}_p + \mathbf{k}_s\,. \tag{3}$$

The vibrational Raman process in crystals involves a coupling between an electromagnetic field and the

---

[1] B. D. Saksena, Proc. Ind. Acad. Sci., Sec. A **12**, 93 (1940).

[2] R. S. Krishnan, Proc. Ind. Acad. Sci. **22**, 329 (1945).

[3] D. Krishnamurti, Proc. Ind. Acad. Sci., Sec. A **47**, 276 (1958).

[4] E. R. Lippincott, A. Van Valkenburg, C. E. Weir, and E. N. Bunting, J. Res. Natl. Bur. Std. (U. S.) **61**, 61 (1958).

[5] I. Simon and H. O. McMahon, J. Chem. Phys. **21**, 23 (1953).

[6] G. Placzek, Akad. Verlagsgesellschaft **2**, 209 (1934).

[7] K. Huang, Proc. Roy. Soc. (London) **208A**, 352 (1951).

[8] A. C. Menzies, Rept. Progr. Phys. **16**, 83 (1953).

[9] R. Loudon, Advan. Phys. **13**, 423 (1964).

TABLE I. Symmetry and matrix elements of vibrations in quartz (Ref. 12).

Group D_3: α-quartz

Symmetry	Vibrations		Nonzero matrix elements	
	Acoustic	Optic	Raman	Infrared
A_1	0	4	α_{zz}' and $\alpha_{xx}'=\alpha_{yy}'$	0
A_2	1	4	0	M_z
E	1	8	$\alpha_{xx}'=-\alpha_{yy}'$ $=\lvert\alpha_{xy}'\rvert$ $\alpha_{xz}'^2=\alpha_{yz}'^2$	$M_x=M_y$

Group D_6: β-quartz

Symmetry	Vibrations		Nonzero matrix elements	
	Acoustic	Optic	Raman	Infrared
A_1	0	1	α_{zz}' and $\alpha_{xx}'=\alpha_{yy}'$	0
B_1	0	3	0	0
A_2	1	2	0	M_z
B_2	0	2	0	0
$E_1(E^-)$	1	4	$\alpha_{xz}'^2=\alpha_{yz}'^2$	$M_x=M_y$
$E_2(E^+)$	0	4	$\alpha_{xx}'=\lvert\alpha_{xy}'\rvert$ $=-\alpha_{yy}'$	0

optical lattice vibrations. If the Hamiltonian density for the crystal is written as $H_{\text{total}}=H_{\text{radiation}}+H_{\text{vibration}}+H_{\text{interaction}}$, then the explicit form of $H_{\text{interaction}}$ is simply $N(\mathbf{P}\cdot\mathbf{E}_e)$ or $N(\boldsymbol{\alpha}\cdot\mathbf{E}_i)\cdot\mathbf{E}_e$, where N is the number of scattering centers per unit volume, $\mathbf{P}$ is the polarization, $\mathbf{E}_i$ is the incident radiation field, $\mathbf{E}_e$ is the scattered radiation field, and $\boldsymbol{\alpha}$ is the polarizability tensor and is assumed in the Placzek model to be a linear function of the normal (vibrational) coordinates:

$$\alpha_{ij}=\alpha_{ij}{}^0+\sum_k q_k\left[\frac{\partial\alpha_{ij}}{\partial q_k}\right]_0, \tag{4}$$

where i, $j=x$, y, or z; $k=1, 2, \cdots, m$ normal modes.

The probability amplitude for a transition via the vibrational Raman effect from state A to state B of an orthonormal basis set is given by

$$(A|H_{\text{int}}|B)=N\sum_l\sum_j\sum_k E_i{}^1E_e{}^j\left(A\left|q_k\left[\frac{\partial\alpha_{1j}}{\partial q_k}\right]_0\right|B\right). \tag{5}$$

The form of the term $\partial\alpha_{ij}/\partial q_k$, which we shall also denote by α_{ij}', will depend only upon the symmetry of the crystal, as is discussed further in the following sections; for each vibration q_k of a symmetric crystal, certain α_{ij}' are zero.

All but one pair of the E^i, E^j components can be set equal to zero experimentally in oriented solids by plane polarizing the incident and scattered radiation. These considerations allow the experimenter to observe all vibrations q_k for which, for example, $\partial\alpha_{xz}/\partial q_k$ is nonzero, and conversely, to find all components α_{ij} for which, say, $\partial\alpha_{ij}/\partial q_3$ is nonzero. This information allows a classification of vibrations into species. The species are determined by the crystal symmetry and are labeled according to the representations of the transformations which preserve elements of crystal symmetry.

Now let us consider the normal modes of the uniaxial crystal quartz. Quartz undergoes a phase change at about 575°C.[10] The low-temperature phase is designated α-quartz; the high-temperature phase, β-quartz. α-quartz is trigonal, of symmetry D_3, and has nine atoms per primitive cell,[11] with the silicon ions at C_2 sites and the oxygen ions at C_1 sites. Group-theory calculations[12] show that the $3N=27$ degrees of freedom are divided into two acoustic vibrations of A_2+E symmetry and sixteen optical vibrations of $4A_1+4A_2+8E$ symmetry, where A_1 vibrations are Raman active, A_2 vibrations are infrared active for the extraordinary ray, and the doubly degenerate E vibrations are both Raman and infrared active (ordinary ray). Selection rules[12] for both α-quartz and β-quartz are indicated in Table I.

β-quartz also has nine atoms per primitive cell, like α-quartz; however, its symmetry is hexagonal D_6,[11] with silicon ions at D_2 sites and oxygen ions at C_2 sites. This results[12] in a division of optical modes into the following symmetries: $\Gamma=A_1+3B_2+2A_2+2B_1+4E_1+4E_2$. The A_1 and E_2 modes are Raman active, A_2 modes are infrared active, E_1 modes are both infrared and Raman active, and type-B vibrations are forbidden for both infrared (electric dipole) and Raman (first-order) effects.

The correlation of modes for α- and β-quartz is[13] shown in Table II.

Even for the α phase, the E vibrations show evidence of E_1 and E_2 characteristics, although this distinction exists formally only for β-quartz. The irreducible representations for E_1, E_2, and E are shown below:

$$\begin{array}{ccc} E_1(D_6) & E_2(D_6) & E(D_3) \\ \begin{bmatrix} 0 & 0 & \alpha_1 \\ 0 & 0 & \alpha_1 \\ \alpha_1 & \alpha_1 & 0 \end{bmatrix} & \begin{bmatrix} \alpha_2 & \alpha_3 & 0 \\ \alpha_3 & -\alpha_2 & 0 \\ 0 & 0 & 0 \end{bmatrix} & \begin{bmatrix} \alpha_2 & \alpha_3 & \alpha_1 \\ \alpha_3 & -\alpha_2 & \alpha_1 \\ \alpha_1 & \alpha_1 & 0 \end{bmatrix}. \end{array}$$

For some of the E vibrations of α-quartz the differential polarizability components α_1 above are much larger than α_3 or α_2; these vibrations show up only weakly or not at all when measurement of α_{xx} or α_{xy} is made. And these are just the vibrations which we expect to be E_1 and infrared active in β-quartz. Similarly, the E vibrations in α-quartz which yield the strongest Raman lines for α_{xx} and α_{xy} measurement should become E_2 vibrations in β-quartz and infrared inactive. Consideration of these effects, in addition to those discussed in the preceding sections, has allowed us to extend our interpretation of the quartz spectrum to the β phase, although the lack of infrared data, especially for

---

[10] P. K. Narayanaswamy, Proc. Ind. Acad. Sci., Sec. A **28**, 417 (1948); the most recent discussion of the phase transition.

[11] W. H. Bragg and R. E. Gibbs, Proc. Roy. Soc. (London) **A109**, 405 (1925).

[12] J. P. Mathieu, *Spectres de Vibration et Symmetrie* (Hermann & Cie., Paris, 1945).

[13] G. Herzberg, *Infrared and Raman Spectra* (D. Van Nostrand Company, Inc., New York, 1945).

β-quartz at wavelengths longer than 15μ and for x-cut samples, does not permit complete analysis and correlation at this time.

In addition to the short-range interatomic forces which predominate in the determination of the vibrational frequencies in crystals, the long-range electric forces influence the frequencies of the longitudinal components of the infrared-active vibrations. These long-range forces affect both frequency and intensity[14,15] of the longitudinal modes, and hence both frequency and intensity can differ from those of the associated transverse mode.

Since the splitting of the species E vibrations in quartz into longitudinal optical (LO) and transverse optical (TO) modes is due to electric forces, the theory appropriate to this discussion is that of the infrared behavior of crystals and not of Raman susceptibilities; if the E vibrations were infrared-inactive, no LO-TO splitting would occur.

Using the model given by Born and Huang[16] and, in particular, Barker's[17] extension of it to crystals with several infrared-active modes, we assume the polarization of a uniaxial crystal having m modes of vibration to be given by

$$P=\alpha_\infty E+\sum_{k=1}^{m} C_k\xi_k(E)\,, \tag{6}$$

where P is the polarization and is treated as a scalar in Eq. (6) under the assumption that $\mathbf{P}$ is parallel to $\mathbf{E}$, E is the strength of the applied electromagnetic field, ξ_k is the amplitude of the kth normal mode and is a function of E, and α_∞ is the value of the polarizability in the high-frequency limit, where the ions cannot follow the oscillation of the field and polarization is entirely due to electron motion.

The assumption of harmonic modes allows us to write, neglecting the phenomenological velocity-dependent damping terms which are sometimes added to explain linewidths,

$$\ddot{\xi}_k+\omega_k^2\xi_k=Z_kE\,,\quad k=1,2,\cdots,m. \tag{7}$$

Here ω_k is the frequency of the k-th normal mode and Z_k is the effective charge coefficient for that mode.

Consideration of plane-wave solutions to Eqs. (6) and (7), i.e., E, P, and ξ all proportional to $\exp[i(\omega t-kp)]$, where $p=z$ or x, y, leads immediately to the expression

$$P=\Big[\alpha_\infty+\sum_{j=1}^{m} C_jZ_j(\omega_j^2-\omega^2)^{-1}\Big]E. \tag{8}$$

Equation (8) allows us to express the dielectric constant, $\epsilon\equiv1+4\pi PE^{-1}$, as

$$\epsilon=1+4\pi\Big[\alpha_\infty+\sum_{j=1}^{m} C_jZ_j(\omega_j^2-\omega^2)^{-1}\Big] \tag{9}$$

or[18]

$$\epsilon=\epsilon_\infty+\sum_{j=1}^{m} S_j\omega_j^2(\omega_j^2-\omega^2)^{-1}\,, \tag{10}$$

where

$$\epsilon_\infty\equiv1+4\pi\alpha_\infty\,,$$

and the mode strength

$$S_j\equiv4\pi C_jZ_j\omega_j^{-2}.$$

Table II. Mode symmetries in quartz.

α-quartz	β-quartz
D_3	D_6
$4A_1$	A_1[a]
	$3B_2$
$4A_2$	$2A_2$
	$2B_1$
$8E$	$4E_1$
	$4E_2$

[a] The species A_1, A_2, B_1, and B_2 have been called A, B, D, and C, respectively, by many earlier authors (including Refs. 1–5). Our notation follows Mathieu (Ref. 12) and Herzberg (Ref. 13).

Equation (10) may be recognized as the equation for the real part of the dielectric constant obtainable from a more general and elegant approach,[19] in which ϵ and S_j are tensors. The simplification from tensor to scalar in the present work and the neglect of the familiar damping constants [assumed zero in Eq. (7)] seems warranted by the nature of the application; the tensor nature of ϵ and S_j requires us to treat z-axis equations separately from x- and y-axis equations, however, even in the simplest approximation.

Note that the definition of mode strength S_j given above has the result that

$$\epsilon(\omega=0)\equiv\epsilon_0=\epsilon_\infty+\sum_{j=1}^{m} S_j\omega_j^2(\omega_j^2-0)^{-1}$$

or

$$\epsilon_0=\epsilon_\infty+\sum_{j=1}^{m} S_j. \tag{11}$$

Now, by imposing Maxwell's equations upon the system and requiring that there be no free charge in the crystal, we have

$$\nabla\cdot\mathbf{D}=0. \tag{12}$$

We now assume homogeneity, which allows us to rewrite

---

[14] R. Loudon, Proc. Roy. Soc. (London) **A275**, 218 (1963).

[15] V. G. Zubov and L. P. Osipova, Kristallografiya **6**, 623 (1962).

[16] M. Born and K. Huang, *Dynamical Theory of Crystal Lattices* (Clarendon Press, Oxford, England, 1954).

[17] A. S. Barker, Jr., Phys. Rev. **136**, A1290 (1964).

[18] An additional term $-\omega_p^2\epsilon_\infty\omega^{-2}$ should be added to the right side of Eq. (10) for the case of crystals with free carriers; here ω_p is the plasma frequency. This term is important in the discussion of LO-plasmon interactions, but is negligible for insulators such as quartz since ω_p^2 is proportional to carrier concentration. See B. B. Varga, Phys. Rev. **137**, A1896 (1965).

[19] D. A. Kleinman and W. G. Spitzer, Phys. Rev. **125**, 16 (1962); M. Lax and E. Burstein, *ibid.* **97**, 39 (1955).

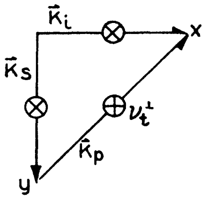

FIG. 1. Vector diagram showing the correlation of photon and phonon propagation and polarization vectors in a crystal of D_3 symmetry. The long arrows denote propagation directions; the short arrows, polarization directions. α_{zz} trace scattering occurs in the xy plane, or $x(zz)y$, (Ref. 21). Only A_1 vibrations will occur for this scattering process. The phonon will have polarization in the z direction and will be $\nu.^{\perp}$

Eq. (12) as

$$\epsilon\nabla\cdot\mathbf{E}=0. \tag{13}$$

Equation (13) has two roots: $\nabla\cdot\mathbf{E}=0$, which implies that $\mathbf{k}$ is perpendicular to $\mathbf{E}$ (transverse modes), and $\epsilon=0$, $\nabla\cdot\mathbf{E}\neq0$, for which $\mathbf{k}$ can be parallel to $\mathbf{E}$, yielding a longitudinal component. The frequencies of these longitudinal modes will, in general, differ from those of the transverse modes in a manner expressed by Eq. (10) for the case $\epsilon=0$. This effect is often referred to as a generalized Lyddane-Sachs-Teller splitting, after the workers who first analyzed it in the case of cubic crystals.[20] The parameters ϵ_∞, S_j (mode strengths) and ω_j (transverse mode frequencies) can usually be determined by dispersion analysis of infrared reflectivity data; for some symmetry species, for example, the E vibrations of α-quartz, the ω_j can also be obtained from Raman studies. Using such S_j and ω_j, one can solve Eq. (10) as an equation in ω. The roots obtained for $\epsilon=0$, $\omega=\Omega_j$, are the longitudinal mode frequencies and should agree with those measured directly in the Raman effect. This is the procedure we have followed in the present work.

It should be stressed that Eq. (10) expresses the coupling between vibrations which have polarization in the same direction. For a uniaxial crystal like quartz there are two sets of equations like Eqs. (7)–(10), one for vibrations which have polarization along the z axis, and one for vibrations which have polarization along the x or y axis. This corresponds to a separation of vibrations into those which are infrared active for the extraordinary ray and those which are infrared active for the ordinary ray, which for α-quartz is just a division into A_2 and E modes, respectively.

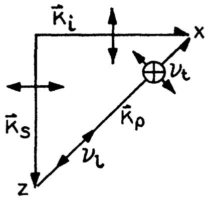

FIG. 3. $x(zx)z$ scattering diagram. Only E vibrations are allowed. One obtains both $\nu_l=[\frac{1}{2}(\nu_l{}^{\perp})^2+\frac{1}{2}(\nu_l{}^{||})^2]^{1/2}$ and $\nu_t=[\frac{1}{2}(\nu_t{}^{\perp})^2+\frac{1}{2}(\nu_t{}^{||})^2]^{1/2}$.

As discussed above, the degenerate E vibrations will each be split into longitudinal and transverse modes of different frequencies, with the transverse frequencies designated ω_j here and the longitudinal frequencies obtained as roots of Eq. (10) for $\epsilon=0$. In addition, the anisotropy of the crystal results in slightly different values for the effective charge coefficients Z_j and also for the C_j [see Eqs. (7)–(10)] for vibrations which propagate parallel or perpendicular to the optic axis. This produces frequencies of vibration, for both transverse and longitudinal modes, which are dependent upon the angle between the optic axis and the direction of phonon propagation.

Consideration of electrostatic effects predicted, for α-quartz, four A_1 unsplit vibrations observable in the Raman effect, four A_2 vibrations observable in the infrared extraordinary ray with frequencies dependent upon orientation, and eight E vibrations, each a doublet in the Raman effect, of which only the transverse component will be infrared active, and in the ordinary ray only. Not every E vibration is expected to have resolvable splitting, but in principle the doubling takes place. The magnitude of the longitudinal-transverse splittings depends critically upon the mode strengths S_j, as can be determined from Eq. (10). Now, in addition to these effects, because of the anisotropy each Raman line can be pure, $\nu^{||}$, pure $\nu^{\perp}$, or a combination,[9,21] such that, assuming electrostatic forces predominate over anisotropy,

$$\nu_l^2=(\nu_l{}^{||}\cos\theta)^2+(\nu_l{}^{\perp}\sin\theta)^2 \tag{14}$$

and

$$\nu_t^2=(\nu_t{}^{||}\sin\theta)^2+(\nu_t{}^{\perp}\cos\theta)^2, \tag{15}$$

where l denotes longitudinal (LO), t denotes transverse (TO), $||$ denotes phonon propagation in the z direction, $\perp$ denotes phonon propagation in the xy plane, and θ is the angle between z (or c) axis and the direction of phonon propagation. Equation (14) and (15), which were derived[9] for a diatomic crystal, are not exact and are based on the assumption that the difference in

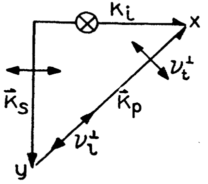

FIG. 2. $x(zx)y$ scattering diagram. Only E vibrations are allowed, both $\nu_l{}^{\perp}$ and $\nu_t{}^{\perp}$.

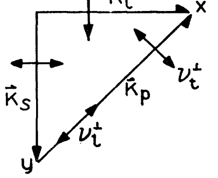

FIG. 4. $x(yx)y$ scattering diagram. Only E vibrations are allowed, both $\nu_l{}^{\perp}$ and $\nu_t{}^{\perp}$.

---

[20] R. H. Lyddane, R. G. Sachs, and E. Teller, Phys. Rev. **59**, 673 (1941).

[21] T. C. Damen, S. P. S. Porto, and B. Tell, Phys. Rev. **142**, 570 (1966).

frequency between longitudinal and transverse vibrations is greater than the frequency difference due to anisotropy, i.e., that

$$|\nu_l^{\perp}-\nu_t^{\perp}|\,,\quad |\nu_l^{\parallel}-\nu_t^{\parallel}|>|\nu_l^{\parallel}-\nu_l^{\perp}|\,,\quad |\nu_t^{\parallel}-\nu_t^{\perp}|\,, \tag{16}$$

and that the difference between the dielectric constants associated with the z and x (or y) axes is small: $|\epsilon^{\parallel}-\epsilon^{\perp}|\ll\epsilon^{\parallel}, \epsilon^{\perp}$. Equation (16) is applicable to some of the vibrations of quartz in the present study; see the following sections. Prior to the present work it had been thought that the inequality in Eq. (16) should be reversed for quartz.[22] For most vibrations in quartz the inequality in Eq. (16) is not a strong one. It depends, unlike the case of the diatomic lattice, upon the particular vibration in question, and need not be generally true for all of the vibrations of a crystal. Because of this, frequencies on the left side of Eqs. (14) and (15) should perhaps not be labeled l or t, since the vibrations to which they refer are partly transverse and partly longitudinal (sometimes designated "quasi-transverse" and "quasilongitudinal"). The 797-cm^{-1} vibration studied by Couture-Mathieu *et al.*[23] is a case where Eq. (16) is a near equality and is an example of the general case mentioned by Loudon.[9] However, for one of the vibrations in α-quartz, the 1072–1235-cm^{-1} doublet, $(\nu_l-\nu_t)$ is more than twenty times as large as $(\nu^{\parallel}-\nu^{\perp})$, and consequently Eqs. (14) and (15) are very good approximations for that case. The validity of the assumptions implicit in applying Eq. (10) to α-quartz with complete neglect of anisotropy is empirically demonstrated in the following sections, which show excellent agreement between observed LO frequencies and those calculated from TO frequencies under the assumption that long-range electrostatic forces predominate over the anisotropy of short-range interatomic forces. While Eq. (10) is found to hold, Eqs. (14) and (15) are probably not applicable to vibrations in α-quartz, except for the 1072–1235-cm^{-1} TO-LO pair.

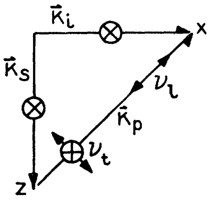

FIG. 5. $x(yy)z$ scattering diagram. Both A_1 and E vibrations are allowed. The A_1 are $\nu=[\frac{1}{2}(\nu^{\parallel})^2+\frac{1}{2}(\nu^{\perp})^2]$, and the E will consist of both

$$\nu_l=[\tfrac{1}{2}(\nu_l^{\perp})^2+\tfrac{1}{2}(\nu_l^{\parallel})^2]^{1/2}$$

and

$$\nu_t=[\tfrac{1}{2}(\nu_t^{\perp})^2+\tfrac{1}{2}(\nu_t^{\parallel})^2]^{1/2}.$$

Figs. 1–7 illustrate the selection rules which result from the combined effects of momentum conservation, symmetry of normal modes and of the polarizability derivative, electrostatic splittings and anisotropy. Note that, as shown in Fig. 7, experimental orientation parameters can be chosen so that the $E(t)$ vibrations are allowed while the $E(l)$ vibrations are completely forbidden for the Raman effect.

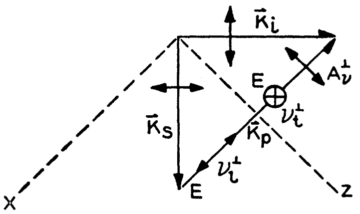

FIG. 6. Diagram for scattering in the xz plane of a 45°-cut crystal. A_1 and E vibrations are allowed. The A_1 are $\nu^{\perp}$ and the E vibrations will consist of $\nu_l^{\perp}$ and $\nu_t^{\perp}$.

EXPERIMENTAL

The Raman spectra of α-quartz were excited with an argon ion laser emitting about 80 mW at 4880 Å. Detection was by means of a Spex 1400 tandem grating spectrometer and a cooled EMI 6256 photomultiplier. Slit widths were 100μ or about 4 cm^{-1}. Signal amplification from the photomultiplier was via a Keithley 610B electrometer. Time constants were about 0.3 sec.

The samples were crystals of about 1 cm per side. The first was cut with one face perpendicular to the c axis, and the second, which we refer to as "45° cut," was cut with the c axis forming the diagonal along one face. Both crystals were cubes. The advantage of the second crystal is that it allowed us to study vibrations in which the direction of phonon propagation was exactly along the c axis or exactly in the ab plane, thus allowing the maximum effect of anisotropy.

Plane-polarized radiation from the laser was focused inside the crystal at normal incidence to one face. Scattered radiation was collected perpendicular to the laser beam and was focused onto the spectrometer entrance slit. A half-wave plate was used to change the direction of incident polarization, and a polarizer was inserted in front of the spectrometer entrance slit to analyze the scattered light.

Figures 8 and 9 show data from the two crystals used. The traces are of the scattering processes denoted by $x(zz)y$ and $x(zx)y+x(yx)y$, where $x(zx)y$ denotes (21) incident and Stokes scattered radiation propagating in the x and y directions, respectively, and incident

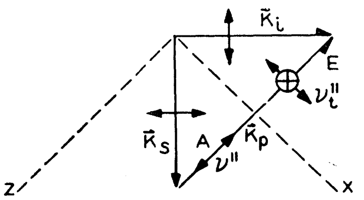

FIG. 7. Diagram for scattering in the xz plane of a 45°-cut crystal. A_1 and E vibrations are allowed. The A_1 are $\nu^{\parallel}$ and the E will consist of $\nu_t^{\parallel}$ only, no $\nu_t^{\perp}$, and, note well, no ν_l, since no E vibrations can have polarization in the z direction. This scattering allows one to eliminate longitudinal E vibrations and thereby identify them.

---

[22] H. Poulet, Ann. Phys. (Paris) **10**, 908 (1955); R. Loudon, Advan. Phys. **13**, 432 (1964).

[23] L. Couture-Mathieu, J. A. A. Ketelaar, W. Vedder, and J. Fahrenfort, J. Chem. Phys. **20**, 1492 (1952).

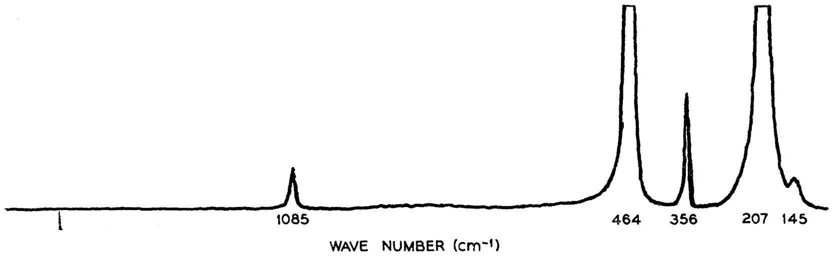

FIG. 8. α_{zz} scattering in α-quartz.

and scattered beam polarizations, respectively, in the z and x directions. In other words, $x(zx)y$ refers to measurement of α_{zx} for a phonon propagating in the xy plane: a ν^1. Figure 8 shows the four A_1 fundamentals and a line of uncertain assignment. Figure 9 shows the eight E vibrations, both longitudinal and transverse components, plus some indication, due to misorientation, of the A_1 line at 464 cm^{-1}. The weak lines marked Ar are argon emission lines from the laser at 5062 Å and 5009 Å.

DISCUSSION

A summary of wave numbers and symmetries of the vibrations observed in the infrared and Raman spectra of α-quartz and β-quartz is given in Table III. The A_2 assignments are those of Spitzer and Kleinman[24]; earlier authors have given different assignments, and, in particular, some argument[3] has been given for the assignment of a vibration at 145–148 cm^{-1} (see Fig. 8) as an A_2 fundamental. We have observed the 145 cm^{-1} vibration in our own Raman study for the α_{zz} scattering. A_2 vibrations are Raman forbidden, and while it might be speculated that this line is an A_2 vibration for which such α_{zz} Raman effect is allowed due to lattice perturbation (strain, etc.), we find such arguments insufficient to refute the assignments and calculations of Spitzer and Kleinman.[18,24] While the nature of the 145-cm^{-1} line is uncertain at this point, it seems fair to say that it is not one of the eight fundamental vibrations. The only infrared study of this spectral region[25] is inconclusive.

TABLE III. Lattice vibrations in quartz.

α-Quartz		β-Quartz[a]	
Species	Wave number (cm^{-1})	Species	Wave number (cm^{-1})
A_1	207	B_2	Forbidden
A_1	356	B_2	Forbidden
A_1	464	A_1	453
A_1	1085	B_2	Forbidden
A_2	364	B_1[b]	Forbidden
A_2	495	A_2	···
A_2	778	B_1	Forbidden
A_2	1080	A_2	···
$E(t)+E(l)$	128	E_2	97
$E(t)+E(l)$	265	E_1	250
$E(t)$	394	E_2	395
$E(l)$	401		···
$E(t)$	450	E_1	···
$E(l)$	509		···
$E(t)+E(l)$	697	E_2	686
$E(t)$	795	E_1	792
$E(l)$	807		···
$E(t)$	1072	E_1	1060
$E(l)+E(t)$	1162	E_2	1154
$E(l)_\perp$	1231		···
$E(l)_\parallel$	1235		

[a] Data from Šimon and McMahon (Ref. 5) and Narayanaswamy (Ref. 10).
[b] Calculated; Narain and Saksena (Ref. 26).

The β-quartz data are those of Šimon and McMahon[5] and Narayanaswamy,[10] but the assignments are ours. The correlation of vibrations of α- and β-quartz apparently has not been understood by some investigators. For example, in an attempt to explain the disappearance of an infrared line upon reaching the transition temperature, Šimon and McMahon have stated[5] that a type-E vibration in α-quartz becomes a type-A vibration in β-quartz. This would imply that a degeneracy is removed, and such is not the case. The phenomenon they observed is due to the fact that the E vibration they studied is one of four which becomes E_2 in β-quartz and is therefore not infrared active at temperatures above 575°C. It does, however, remain a doubly degenerate vibration; no degeneracies are removed by the $\alpha\beta$ transition in quartz.

The E_1 and E_2 assignments given in Table III are not certain in all cases and could be confirmed by infrared studies on β-quartz at long wavelengths or by polarized Raman studies of β-quartz, neither of which have been performed yet. Our assignment is most certain in the case of the E_2 line at 1154 cm^{-1}, which vanishes entirely in the infrared[5] in going through the transition temperature but remains undiminished in the Raman effect.[10] Theoretical calculations by others,[26] however, have predicted that this 1154-cm^{-1} line is E_1, which shows the inaccuracy of force-constant calculations for the E vibrations. The force-constant calculations for A_2 and B_1 vibrations of β-quartz involve only quadratic equations in ω^2 and are more reliable than those for E_1 and E_2 vibrations, which involve quartic equations. The former appear to be fairly accurate, and we have used them to determine which A_2 modes of α-quartz remain A_2 in β-quartz and which become B_1, in lieu of infrared data on x-cut β-quartz.

---

[24] W. G. Spitzer and D. A. Kleinman, Phys. Rev. **121**, 1324 (1961).

[25] E. K. Plyler and N. Acquista, J. Opt. Soc. Am. **45**, 900 (1955).

[26] B. D. Saksena and H. Narain, Proc. Ind. Acad. Sci., Sec. A **30**, 128 (1949).

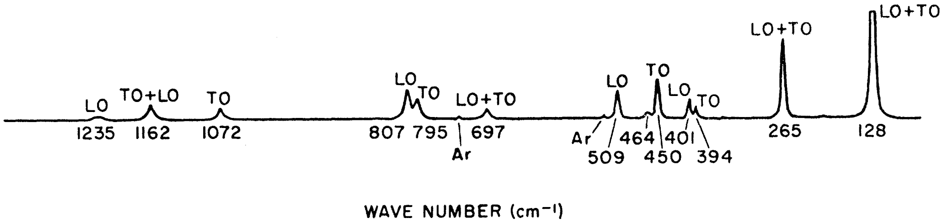

FIG. 9. $(\alpha_{xz}+\alpha_{xy})$ scattering in α-quartz.

All of our E_1 and E_2 assignments for β-quartz have been made on the basis of the relative strengths of the corresponding transition in α-quartz for α_{xy} and α_{xz} scattering, as discussed earlier in the text, with the assumption that α-quartz E modes with $a_{xy} \gg \alpha_{xz}$ become E_2 modes in β-quartz; this is supported by the small amount of existing infrared data on β-quartz. Our assignments differ from those of Refs. 26 and 27 (normal-mode analyses), which also disagree with each other. Kleinman and Spitzer[18] have suggested an alternative method of assigning the E_1 and E_2 vibrations of β-quartz; they observed that four of the eight E vibrations in α-quartz are only weakly infrared active and proposed that these are the four which become E_2 and infrared inactive in β-quartz. In every case but one these E_2 assignments of Kleinman and Spitzer agree with ours; the single difference is that their assignment would reverse that given in Table III for the 250- and 395-cm^{-1} bands of β-quartz. An infrared study of β-quartz from 25 to 40 μ would resolve the question.

The E_1 lines of β-quartz should show transverse-longitudinal electrostatic splittings, like the E lines of α-quartz; however, the available Raman data[10] show no "extra" lines attributable to longitudinal E_1 components.

The $E(l)$ or LO assignments for α-quartz are ours. Most earlier workers attributed these lines to multiphonon processes and devised elaborate assignment schemes. Mathieu and Couture-Mathieu[28] correctly supposed that the 394–401- and 795–807-cm^{-1} doublets consist of a transverse vibration at the lower frequency and a longitudinal vibration at the higher frequency, but they were unable to account quantitatively for the splittings and were erroneous in assigning the 1235-cm^{-1} line as an unresolved transverse-longitudinal doublet; we show (see Table IV) that it is the longitudinal component associated with the transverse mode at 1072 cm^{-1}.

Table IV compares the observed and calculated frequencies of the longitudinal components of the E vibrations of α-quartz. Calculated values were obtained by inserting the values of ω_j from our own measurement of the transverse vibrations and ϵ_∞ and S_j from Spitzer and Kleinman[24] and Barnes[29] (infrared dispersion analysis) into Eq. (10) for the case $\epsilon = 0$. S_j for the 128- and 265-cm^{-1} lines reported by Barnes were taken as the same as that for the 697-cm^{-1} line on the basis of a qualitative comparison given by Spitzer and Kleinman. We have neglected anisotropy in this calculation. Observed and calculation values agree very well in each case, in view of our 2–3-cm^{-1} resolution.

Since the anisotropic shifts are of the same magnitude as our spectral resolution, we were able to make quantitative measurements in very few cases. The maximum relative shift due to anisotropy occurs for comparison of phonon propagation along z and along x, and for α-quartz this shift is largest for the longitudinal vibration at 1235 cm^{-1}. However, for longitudinal E vibrations, propagation along z is forbidden (see Fig. 7), so the maximum frequency shift observable is in practice somewhat less for α-quartz than that which exists in principle. Our estimation of the full anisotropic shift for the 1235-cm^{-1} line is 3 cm^{-1}, which is about the same as that reported by Mathieu and Couture-Mathieu.[28] The anisotropy was apparent in the α_{xz} scattering in our work for phonon propagation along the x axis and for phonon propagation in the xz plane at 45° to the z axis. The frequency shift between these two cases was observed in our work to be about 1.5 cm^{-1}, with the lower frequency corresponding to propagation along x, i.e., for $\nu_l{}^{\perp}$. This shift should be about half the difference between $\nu_l{}^{\perp}$ and $\nu_l{}^{\parallel}$ [see Eqs. (14) and (15)], and so if the longitudinal vibrations were permitted for which the phonon propagates along z, it should be about 3 cm^{-1} higher in frequency than for that along x.

Birefringence and optical activity are well-known effects in quartz. They undoubtedly created problems of interpretation in the early work with oriented samples. For example, consider the scattering process

TABLE IV. Transverse and longitudinal vibrations in α-quartz of symmetry species E (cm^{-1}).

Observed transverse	Observed longitudinal	Calculated longitudinal[a]
128±2	128±2	128.3
265	265	265.5
394	401	402.7
450	509	508.7
697	697	699.1
795	807	807.8
1162	1162	1159.9
1072	1235	1236.8

[a] Calculated using Eq. (10) with the ω_i transverse frequencies measured in the present work and given above, S_i and ϵ from Ref. 24, and S_i for the lines at 128 and 265 cm^{-1} taken as ~0.02 from a qualitative comparison of strengths in Refs. 24 and 27.

---

[27] J. Barriol, J. Phys. Radium **7**, 209 (1946).

[28] J. P. Mathieu and L. Couture-Mathieu, Compt. Rend. **234**, 1961 (1952).

[29] R. B. Barnes, Phys. Rev. **39**, 562 (1932).

denoted by $z(yx)y$, which should yield only the E vibrations. However, due to the optical activity, after travelling a small distance into the crystal the incident light will not be y polarized, but will have polarization intermediate between x and y. The resulting x component of the incident field will necessitate simultaneous measurement of $z(yx)y$ and $z(xx)y$ and will allow the A_1 vibrations to be seen also. To avoid this complication we made, for example, measurement of α_{yx} scattering in the present work by means of the orientation given by $x(yx)y$. Such measurements allow complete discrimination between A_1 and E vibrations.

Unfortunately, birefringence continues to be neglected in experimental work even today. Kiselev and Osipova have failed to consider this effect properly in their most recent work.[30] As a result, they found for α-quartz a value $\alpha_{xy}/\alpha_{yy}=4$–$5\%$ for the 466-cm^{-1} A_1 line. Theoretical considerations dictate that α_{xy} should be exactly zero for A_1 vibrations. We examined the 466-cm^{-1} region for α_{xy} and α_{yy} scattering, in particular, for $y(xy)x$ and $x(yy)z$, and found the relative intensities of the 466-cm^{-1} line to be $\ll 1\%$. certainly not of the order of 4%, and well within the limits expected from slight crystal misorientation or wandering of the z axis. Indeed, Raman emission at 466 cm^{-1} for $y(xy)x$ scattering was only barely perceptible. We conclude that the computer fit to α_{ij} for A_1 lines given by Kiselev and Osipova is not very meaningful. An explanation of and correction for such depolarization errors as are present in Kiselev and Osipova's work has been given by Giordmaine *et al.*[31]

As an additional comment, we wish to point out that our assignment of the vibration at about 1235 cm^{-1} as the longitudinal component of the E vibration which has its transverse component at 1072 cm^{-1} seems certain. We were unsuccessful in our attempts to resolve the predicted doublet at 1162 cm^{-1}. It should appear unusual when resolved and studied with a 45°-cut crystal in that it should consist of a longitudinal vibration at a slightly *lower* frequency than the nearby transverse (normally the effect of electrostatic forces is to shift the LO to a slightly higher frequency compared to the TO). This situation is due to the fact that an E vibration occurs at 1162 cm^{-1} in α-quartz, *between* the TO and LO components of another vibration of the same symmetry, and due to the mathematical requirement that an LO must occur at a frequency between every pair of TO's, for a given symmetry species.

Our assignment of the 1235- and 509-cm^{-1} lines raises the question of the occurence of resonances at about 1225 and 509 cm^{-1} in the infrared reflectivity data.[24] Since our observed positions of 1235 and 509 cm^{-1} agree very well with our calculated values, and since we were able to make these lines disappear for scattering in which the phonon propagates along the z axis, these two Raman lines are unquestionably E longitudinal and nothing else. The appearance of resonances at about these frequencies in infrared data *could* be a coincidence, but no evidence is available at present to suggest that they are binary combination bands (two-phonon processes).

It seems at least equally likely to us that the observed phenomenon is a case of electrostatic forces predominating over the crystal field splitting. There are four pairs of vibrations in α-quartz which consist of an A_2 and an E vibration close in frequency; in the cubic approximation each of these pairs would be a triply degenerate vibration. For only two of these cases the A_2 vibration lies at a frequency slightly higher than the E transverse and hence occurs at a frequency between that of the E transverse and the E longitudinal. These two E longitudinal vibrations are the two which appear to be infrared-active in the extraordinary ray[24] and hence to evidence A_2 characteristics. The frequencies of the vibrations in question are 450, 495, 509 cm^{-1} in the first case and 1072, 1080, 1235 cm^{-1} in the second case for $E(t)$, A_2, $E(l)$ vibrations, respectively. The observations are suggestive of mixed $A_2+E(l)$ character for the two vibrations at 509 and 1235 cm^{-1}. Of the infrared resonances at 509 and approximately 1225 cm^{-1}, the former is very much the stronger, which is consistent with its nearness to the 495-cm^{-1} A_2, if the mixing hypothesis is correct. No formalism for the discussion of this hypothesis will be presented here.

In summary, it appears that α-quartz provides a physical system in which the effects due to electrostatic forces, anisotropy of short-range forces, and splittings introduced by the noncubic crystal field are all of comparable magnitude. As such, it should provide fertile ground for more detailed calculations in the future and should be an ideal material for the study of the optical properties of the most general uniaxial crystal.

ACKNOWLEDGMENTS

The authors would like to acknowledge the careful experimental work of L. E. Cheesman, who obtained the Raman data used in this work, and to thank Mrs. M. L. Thomson, who programmed the solution to Eq. (10), and A. Albert, who prepared the quartz samples. We appreciate discussions on the subject with Dr. B. Tell, Dr. R. P. Bauman, Dr. D. A. Kleinman, Dr. J. P. Gordon, and others who provided comments on the manuscript. The use of lasers provided by E. I. Gordon and R. C. Miller is also gratefully acknowledged.

---

[30] D. F. Kiselev and L. P. Osipova, Kristallografiya **11**, 357 (1966).

[31] S. P. S. Porto, J. A. Giordmaine, and T. C. Damen, Phys. Rev. **147**, 608 (1966).